Orthogonal Vector Approach for Reducing Loadpulling Effect in MIMO Transmitters

Orthogonal Vector Approach for Reducing Loadpulling Effect in MIMO Transmitters

Jiayu hou#1, Haijun Fan#2, Yuan Ding#3, George Goussetis#4

#Institute of Sensors, Signals and Systems (ISSS), Heriot-Watt University, UK
{1jh2064, 2h.fan, 3yuan.ding, 4g.goussetis}@hw.ac.uk

***Abstract* — In this paper, we propose a low complexity precoding method that is based on orthogonal vector (OV) concept in order to mitigate power amplifier (PA) loadpulling effect in a highly integrated transmitter (Tx) antenna array. The precoder is designed by summing an excitation vector that is orthogonal to the channel state information (CSI) to the conventional zeroforcing (ZF) precoder. In this way the equal constant power (CP) signals can be synthesized and injected into all PAs at each time instant, in the meantime the orthogonality ensures that the additive vector has no impact on the signal at the intended receiver (Rx). The simulations have been performed, and it shows that the proposed precoder can reduce the loadpulling effect with a low complexity algorithm.**

***Keywords* — highly integrated array, loadpulling effect, orthogonal vector (OV), power amplifier (PA).**

I. Introduction

In order to achieve an increased channel/network capacity, a significant number of antenna elements are being equipped in the next generation cellular networks. The resulting massive-multiple input and multiple output (m-MIMO) systems call for an integrated transmitter (Tx) architecture due to its benefits of reduced hardware complexity and the associated cost and energy consumption [1]. In the compact integrated Tx, the unavoidable antenna crosstalk/coupling, unfortunately, will cause active loadpulling effect for power amplifiers (PAs) whose outputs are exposed to non-isolated antenna arrays [2]. As an explanation, each PA in the radio frequency (RF) chain at Tx will experience a wave injected to its output port, which is a superposition of the mismatch reflection from the directly connected antenna and the coupling from all the other antennas nearby. This interaction between the antenna array and the PAs renders each PA see a dynamic non-50 Ω load. This PA loadpulling effect has been shown to generate non-negligible interference that compromises signal fidelity and system performance [2]–[3].

The PA loadpulling effect has recently caught wide attention with a lot of efforts in recently reported works [4]–[8]. Digital predistortion (DPD) is a matured and conventional technology for PA linearization, and one of its variants, namely dual input-DPD (DI-DPD) [4]–[6], was proposed for compensating PA loadpulling effect. However, the DI-DPD algorithm was too complicated to be applied to an array with a huge number of antenna elements. In [7]–[8], new precoders, with an extra constraint on equal average transmit power across array elements, were proposed. It experimentally proved that this statistic method based on numerical optimization could effectively reduce the PA dynamic impedance variation, i.e., the size of the area on Smith chart within which the PA active impedances are scattered when transmitting dynamic modulated signals. However, the procedure for solving the precoder can be tedious as the algorithm complexity would increase when the Tx antenna array size is huge.

Building upon the findings in [7] and inspired by the orthogonal vector (OV) approach in [9], we propose to apply this OV method to reduce the PA loadpulling effect in coupled highly integrated antenna arrays. In particular, we will show in this paper that the PA loadpulling effect at Tx can be suppressed by injecting deterministic equal constant power (CP) signals to all PAs at any time instant, and such signals can be synthesized with low complexity.

The rest of this paper is organized as follows; The system model is presented in Section II, together with the analysis for the conventional zeroforcing (ZF) precoded signal under the coupled Tx antenna array. The proposed OV based CP precoder is also introduced in Section II. The simulation validation for the proposed precoder that alleviates loadpulling effect is presented in Section III along with the algorithm complexity analysis. Finally, the conclusion and future works are summarized in Section IV.

Notations used in this paper are listed as follows; The transpose and pseudo-inverse are denoted as $[\cdot]^T$ and $(\cdot)^{-1}$, respectively. The operator $|\cdot|$ returns the magnitude of the enclosed complex number. The notation diag$\{\cdot\}$ refers to a diagonal matrix. Letters in bold represent matrices or vectors.

II. Constant Envelope Signal Generation with Orthogonal Vector

A. System Model

A single-user MIMO (SU-MIMO) system to be studied in our work is illustrated in Fig. 1. The system consists of a Tx array with N antenna elements and a receiver (Rx) equipped with a single antenna. Each Tx antenna is served by a dedicated RF chain with a PA directly connected to the antenna. The multi-path wireless propagation channel is assumed in our work, and its channel state information (CSI) is represented by a $1\times N$ vector $\boldsymbol{H}$ with its n^{th} element of h_n, where $n = 1, 2, \ldots, N$. We label the PA connected to the n^{th} antenna element as PA_n. Seen in Fig. 1, the signal waves injected into the input and output ports of the PA_n are denoted as a_{1n} and a_{2n}, respectively; b_{2n} refers to the transmitted wave at the output port of the PA_n (from PA to the antenna). The

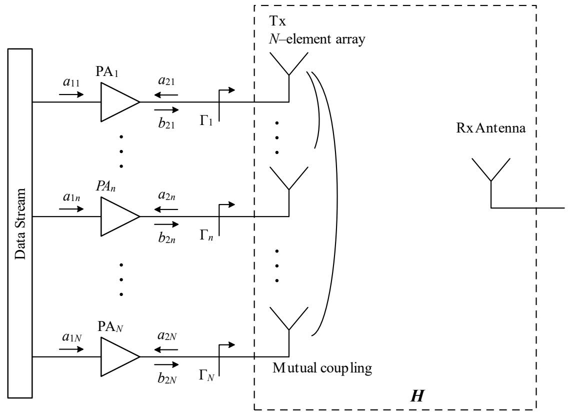

Fig. 1. An SU-MIMO link model studied in this paper.

input and output signal vectors of PAs in Tx are expressed as $\boldsymbol{A}_1 = [a_{11}, \ldots, a_{1n}, \ldots, a_{1N}]^T$ and $\boldsymbol{B}_2 = [b_{21}, \ldots, b_{2n}, \ldots, b_{2N}]^T$, respectively. The relation between $\boldsymbol{A}_1$ and $\boldsymbol{B}_2$ is

$$\boldsymbol{B}_2 = \boldsymbol{G}\boldsymbol{A}_1. \tag{1}$$

Here $\boldsymbol{G}$ is a diagonal gain matrix defined as $\boldsymbol{G} = \mathrm{diag}\{g_1, \ldots, g_n, \ldots, g_N\}$, with g_n representing the gain of the PA_n. The value of g_n is dependent on the active reflection coefficient, Γ_n, seen by the PA_n. This Γ_n can be calculated as

$$\Gamma_n = \frac{a_{2n}}{b_{2n}} = \frac{1}{b_{2n}} \sum_{m=1}^{N} S_{nm} b_{2m} , \tag{2}$$

where S_{nm} is the $\{n, m\}^{\text{th}}$ entry in the scattering matrix $\boldsymbol{S}$ of the Tx antenna array, and $m = 1, 2, \ldots, N$.

In order to facilitate the study in this paper, the assumptions have been made as below;

- Only Tx knows full CSI.
- Each PA is perfectly matched at its input port, i.e., no reflection at all PA input ports.
- PA gain compression at each fixed load is linearized, and our study will focus on the influence of PA loadpulling effect.

B. *Conventional Zeroforcing Precoder*

When the conventional ZF precoder is applied, the baseband equivalent signal at PA input is

$$\boldsymbol{A}_{1,ZF} = \boldsymbol{W}_{ZF}\, s. \tag{3}$$

The subscription 'ZF', and 'CP' appearing later in the paper, refer to the conventional ZF and our proposed OV based CP methods. s is the symbol to be transmitted. Note that for simplicity we have omitted the notation for the time index. $\boldsymbol{W}_{ZF}$ in (3) is the ZF precoding vector, which is obtained by

$$\boldsymbol{W}_{ZF} = \boldsymbol{H}^{-1}. \tag{4}$$

The received signal at Rx can be written as

$$y_{\mathrm{ZF}} = \boldsymbol{H}\boldsymbol{B}_{2,ZF} = \boldsymbol{H}\boldsymbol{G}_{ZF}\boldsymbol{W}_{ZF}\, s + \sigma, \tag{5}$$

where σ represents additive white Gaussian noise (AWGN). When the system is isolated, the amplification matrix $\boldsymbol{G}_{ZF}$ is an identity matrix multiplied with a complex constant, the PA small signal gain g_{ss}. Thus, the received signal becomes

$$y'_{\mathrm{ZF}} = g_{ss}\, s + \sigma. \tag{6}$$

Unfortunately, when antennas are clustered together and are exposed to PA outputs, the active loadpulling effect results in discrepancies among the values of each diagonal element in $\boldsymbol{G}_{ZF}$. This inevitably leads to distortion to the symbol s. This will eventually compromise the link throughput. It has been studied in [7] that when the transmit power difference among coupled antennas is minimized, the PA loadpulling effect can be reduced. Following the similar principle, we propose a low complexity method to reduce the active reflection coefficient variation to a similar level by synthesizing OV based CP signals.

C. *Our Proposed Orthogonal Vector Based Constant Power Precoder*

In order to compensate for the signal power variation among all the Tx chains, we propose to add an $N\times1$ signal vector $\boldsymbol{V} = [v_1, \ldots, v_n, \ldots, v_N]^T$ to the conventional ZF precoder to construct a new precoder for CP signals at input ports of all PAs. Mathematically this is expressed as

$$\boldsymbol{A}_{1,CP} = (\boldsymbol{W}_{ZF} + \boldsymbol{V})\cdot s, \tag{7}$$

which satisfies

$$|a_{1n,\mathrm{CP}}| = p,\ \forall n \in \{1, 2, \ldots, N\}. \tag{8}$$

Ensuring the extra added excitation vectors not affecting the received signals at the intended Rx is critical. In our method this is guaranteed that $\boldsymbol{V}$ is orthogonal to the CSI $\boldsymbol{H}$, namely,

$$\boldsymbol{H}\boldsymbol{V} = 0. \tag{9}$$

The received signal in the CP system is

$$y_{\mathrm{CP}} = \boldsymbol{H}\boldsymbol{B}_{2,CP} = \boldsymbol{H}\boldsymbol{G}_{CP}\,(\boldsymbol{W}_{ZF} + \boldsymbol{V})\cdot s + \sigma. \tag{10}$$

When the CP system is isolated, the received signal would be the same as that in the isolated conventional ZF system.

$$y'_{\mathrm{CP}} = y'_{\mathrm{ZF}} = g_{ss}\, s + \sigma \tag{11}$$

In Fig. 2 an illustrative graphic explanation is presented to facilitate understanding of the proposed OV based CP method. Fig. 2(a) indicates how the received signals in the I-Q plane are contributed by the signals radiated by each Tx antenna. In this example, $N = 4$ is used. Fig. 2(b) is a geometry expression for (9), which demonstrates the orthogonality between the vector $\boldsymbol{V}$ and the CSI $\boldsymbol{H}$ and elucidates why the two trajectories in Fig. 2(a) coincide at the target symbol. The designed trajectories in Fig. 2(a) are synthesized by assuming that all PAs provide a unit one, and the PAs input signal vector is thus the same as the output vector. However, the actual trajectories would deviate from the designed paths because of the loadpulling effect.

The synthesis procedures of the OV based CP signals are not elaborated in two steps.

Step 1. Determine the CP signal power.

To ensure the solutions for $\boldsymbol{V}$ satisfying (8) and (9) exist, there need two constraints as shown in (12) and (13), so as to avoid the cases shown in Fig. 3(a) and (b) respectively. In these two cases the ending point of the trajectories cannot reach the target symbol in the Rx I-Q plane.

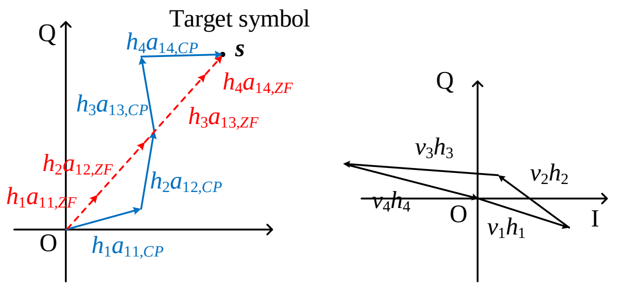

(a) (b)

Fig. 2. At the Rx I-Q plane, (a) ZF signals in dash lines and CP signals in solid lines; (b) the OV excitation radiated by a 4-element Tx array, transmitted through the channel then received at Rx.

$$p\left(2\cdot\max\left(|h_1|,\cdots,|h_N|\right)-\sum_{n=1}^{N}p|h_n|\right)\leq|s| \tag{12}$$

$$p\cdot\left(\sum_{n=1}^{N}|h_n|\right)\geq|s| \tag{13}$$

By solving (12) and (13) the range of the transmitted signal power can be found. The value p can be selected within this feasible range, and the selection will not affect received signal power as $\boldsymbol{V}$ is orthogonal to $\boldsymbol{H}$. Selecting different p for different channels or even different symbols is also supported. The system energy efficiency is mainly determined by p. To illustrate, for the same channel and same symbol, the larger p indicates more extra energy is injected into the system for compensating loadpulling effect, with reduced energy efficiency. Note that as long as p is in the range determined by (12) and (13), the OV can be synthesized which has no impact on received signals.

Step 2. Find a solution for $\boldsymbol{V}$.

Once p is selected, the signal v_n added to the n^{th} Tx chain can be calculated. It is easy to understand that the ending point of the trajectory C_n, see (14), on the Rx I-Q plane must be on a circle centered at C_{n-1} when $n > 1$, or centered at the origin when $n = 1$, with the radius of $|ph_n|$.

$$C_n=\sum_{m=1}^{n}a_{1m,CP}\cdot h_m \tag{14}$$

When determining $a_{1n,CP}$, it needs to be ensured that the remaining signal vectors will not fall into the cases illustrated in Fig. 3, thus,

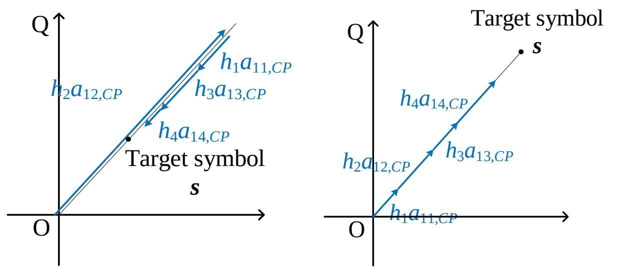

(a) (b)

Fig. 3. Two cases that give no solutions to (8) and (9). These can be avoided by applying the constraints for p stated in (12) and (13). N = 4 is assumed in this example.

$$p\left(2\cdot\max\left(|h_{n+1}|,\cdots,|h_N|\right)-\sum_{m=n+1}^{N}p|h_m|\right)\leq|C_n-s|, \tag{15}$$

$$p\cdot\left(\sum_{m=n+1}^{N}|h_m|\right)\geq|C_n-s|. \tag{16}$$

The conditions in (15) and (16) also give a set of $a_{1n,CP}$, and a corresponding set of v_n. The solutions for $\boldsymbol{V}$ are not unique.

III. Simulation Validation

To validate the proposed OV based CP precoder design can effectively suppress the PA active reflection coefficient variations, we perform a virtual 16QAM transmission link through 1,000 random Rayleigh channel realizations. The system operates at 3.5 GHz. A 4×4 capacitive-fed patch antenna array is simulated and is used for Tx, whose dominant coupling is −19.7 dB. The simulated active reflection coefficients are presented in Fig. 4 for 4 out of 16 selected PAs. Since the array is symmetric, the 4 typical elements, indexed as 1, 3, 6, and 11, are chosen, see inset in Fig. 4. The active reflection coefficient distributions under 3 different precoding approaches are also compared in Fig. 4, with blue stars for the conventional ZF precoder, red dots for the EP-RZF precoder described in [7], and the yellow dots for our proposed OV based CP precoder.

Observing from Fig. 4, both the proposed OV based CP precoder and EP-RZF precoder introduced in [7] could mitigate the loadpulling effect compared to the conventional ZF precoder. They can confine the active reflection coefficients to a much smaller region in the Smith chart. However, our proposed method in this paper enjoys low computation complexity. The signal vector $\boldsymbol{V}$, to be synthesized in our method, only has N parameters to be determined. Whereas the algorithm adopted for the EP-RZF

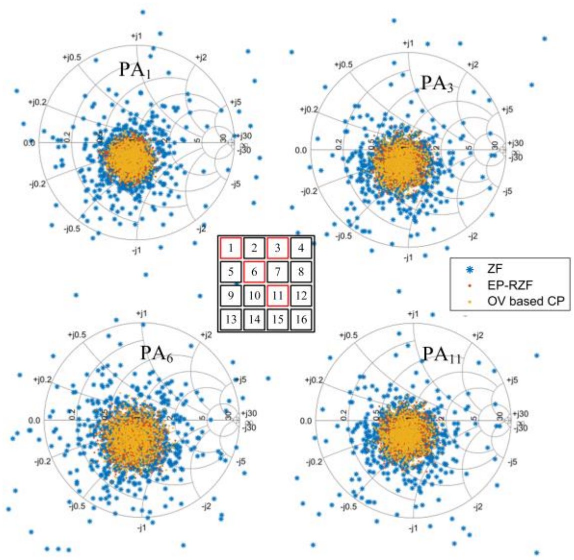

Fig. 4. Simulated active reflection coefficients in the conventional ZF, the EP-RZF precoder [7], and our proposed OV based CP methods. 4 typical chains are chosen in a 4×4 Tx array.

method in [7] needs to solve for (2N+1) parameters. Unlike the proposed OV approach, where the precoder can be generated by using adding and multiplication, the precoding method in [7] needs differentiation and matrix inverse calculation which results in a significantly higher algorithm complexity. Apart from the complexity benefit, our proposed precoding method can dynamically adjust the system power efficiency by selecting different values of p.

IV. Conclusion and Future Work

In this work, an equal power signal generation based on the additive OV was introduced. This proposed CP signal generation method could effectively reduce the PA loadpulling effect in a non-isolated MIMO Tx. The next step will be extending this proposed OV based CP precoder for the multi-user scenario, as well as the experimental validation in practical field tests.

Signal magnitude is not the only factor that influences the PA loadpulling effect, the signal phase variation among all Tx chains also plays an important role. This indicates that the CP signals cannot fully eliminate the PA loadpulling effect. Consequently, novel signal waveform designs are required to further suppress the PA loadpulling effect and optimize the entire system performance. Our research in this aspect will be reported in our future work.

Acknowledgment

This work was supported by UK Engineering and Physical Sciences Research Council under the Grant EP/V002635/1. For the purpose of open access, the authors have applied a Creative Commons Attribution (CC BY) license to any Accepted Manuscript version arising.

References

[1] R. Hussain and M. S. Sharawi, "5G MIMO antenna designs for base station and user equipment: Some recent developments and trends," *IEEE Antennas Propag. Mag.*, vol. 64, no. 3, pp. 95–107, Jun. 2022.

[2] C. Fager, T. Eriksson, F. Barradas, K. Hausmair, T. Cunha, and J. C. Pedro, "Linearity and efficiency in 5G transmitters: New techniques for analyzing efficiency, linearity, and linearization in a 5G active antenna transmitter context," *IEEE Microw. Mag.*, vol. 20, no. 5, pp. 35–49, May 2019.

[3] H. Fan, Y. Ding, G. Goussetis, and M. J. C. Sanchez, "Antenna array driven by non-isolated power amplifiers for MIMO applications", in *Proc. 49th Eur. Microw. Conf. (EuMC)*, pp. 468–471, Oct. 2019.

[4] C. Fager, X. Bland, K. Hausmair, J. Chani Cahuana, and T. Eriksson, "Prediction of smart antenna transmitter characteristics using a new behavioral modeling approach", in *Proc. IEEE MTT-S Int. Microw. Symp.*, pp. 1–4, 2014.

[5] H. Zargar, A. Banai, and J. C. Pedro, "A new double input-double output complex envelope amplifier behavioral model taking into account source and load mismatch effects," *IEEE Trans. Microw. Theory Tech.*, vol. 63, no. 2, pp. 766–774, Feb. 2015.

[6] K. Hausmair, P. N. Landin, U. Gustavsson, C. Fager, and T. Eriksson, "Digital Predistortion for Multi-Antenna Transmitters Affected by Antenna Crosstalk," *IEEE Trans. Microw. Theory Tech.*, vol. 66, no. 3, pp. 1524–1535, Mar. 2018.

[7] M. Almoneer, J. G. Lim, H. Yu, P. Mitran, and S. Boumaiza, "Massive MIMO precoding methods that minimize the variation in average power and active impedance with channel conditions," *IEEE Trans. Microw. Theory Tech.*, vol. 70, no. 8, pp. 4002–4016, Aug. 2022.

[8] A. B. Ayed, P. Mitran, and S. Boumaiza, "Novel algorithm to synthesize the tapering profile for enhanced linearization of RF beamforming arrays over a wide steering range," *IEEE Trans. Microw. Theory Tech.*, vol. 71, no. 8, pp. 3691–3700, Aug. 2023.

[9] J. M. Purushothama, Y. Ding, G. Goussetis, G. Huang, and Y. Xiao, "Synthesis of energy efficiency-enhanced directional modulation transmitters," *IEEE Trans. Green Comm. Netw.*, vol. 7, no. 2, pp. 635–648, Jun. 2023.